Progress In Electromagnetics Research Letters, Vol. 11, 139–148, 2009

$BaZrO_3$:Yb NANOPHOSPHOR FOR EFFICIENT UP-CONVERSION LIGHT EMISSION

L. A. Diaz-Torres, E. de la Rosa, and J. Oliva

Centro de Investigaciones en Optica A.C.
Leon, Gto. 37150, Mexico

P. Salas and V. M. Castaño

Centro de Física Aplicada y Tecnología Avanzada
Universidad Nacional Autónoma de México
Boulevard Juriquilla 3001, Querétaro 76230, Qro. Mexico

Abstract—Strong visible green upconversion emission in nanocrystalline $BaZrO_3$:Yb^{3+} powder, obtained by a hydrothermal process at 100°C, is reported. The unconverted emission has a quadratic dependence on the pump intensity with a lifetime around half that of the NIR lifetime. Results suggest cooperative upconversion as the mechanism responsible for the green fluorescence. This efficient Yb^{3+}-based cooperative up-conversion process allows the development of novel emitting materials in the ultraviolet to visible (UV-VIS) range.

1. INTRODUCTION

Frequency up-conversion phenomena in trivalent Rare-Earth (RE) ions, hosted in a number of matrixes, have been widely investigated in the past two decades, due to their potential use as visible-wavelength luminescent materials [1–11]. Indeed, Yb^{3+}-based up-conversion phosphors are thought for applications ranging from biotechnology [1, 2] to high power lasers [3–5]. Since inexpensive near-infrared (NIR) pump sources, such as solid-state lasers and semiconductor laser diodes, are readily available nowadays, all kinds of NIR-to-visible up-conversion emissions and various energy-transfer processes based on the use of Yb^{3+} have been investigated [6–9]. Recently, detailed reviews involving Yb^{3+} as the base of up-conversion processes in solids have been published by Auzel [10]

Corresponding author: L. A. Diaz-Torres (ditlacio@cio.mx).

and Gudel et al. [11]. More specifically, improved functionality related to Yb^{3+} in a nanosized host appears to be a promising area of research [12, 13]. Particularly active is the search of new host materials with small multiphonon decay rates and good structural and chemical stability over a wide range of temperatures and corrosive environments. Perovskite materials have attracted vast attention due to their excellent optical, electrical, chemical properties and capability of hosting functional ions of various sizes [14–16]. In particular, oxides such as $YAlO_3$, $BaTiO_3$, $LiNbO_3$, and fluorides such as $KMgF_3$ and $NaYF_4$ have found important applications in visible-emitting phosphors when hosting Er and Yb ions [11, 17–20]. Oxides are quite resistant to corrosive environments and have good optical properties. However, most perovskites present phase transformations that lead to anisotropies in their refraction index, which causes non-linear optical phenomena such as second harmonic generation. For some high-energy upconversion applications, this represents a limiting factor, since the upconversion-generated heat can induce anisotropies, thus limiting the effective range of pumping power.

Barium zirconate ($BaZrO_3$) is a very promising refractory structural material with a very high melting point (2920°C) and low chemical reactivity with corrosive compounds like the ones used in the fabrication of high temperature superconductors. Among the cubic oxide perovskites, $BaZrO_3$ (BZO) is the only one that does not follow phase transitions over the range from 1600 K down to 4 K [21]. Recently, columnar inclusions of BZO nanocrystallites were found to enhance the transport currents in YBCO superconductors [22]. Additionally, BZO has attracted attention as a promising candidate for protonic electrolytes in fuel cell applications [16]. Here, we report the NIR and visible (VIS) emission properties of nanocrystallites of Yb^{3+}-doped BZO (BZO:Yb), as powders synthesized by simple hydrothermal method. The strong green upconversion luminescence of BZO:Yb makes it a feasible candidate for visible light generation via upconversion processes and, therefore, suitable for biological labeling under NIR excitation [1, 2].

BZO powders, both as-prepared and doped with Yb^{3+} 0.1, 0.5, 1.0, 2.5, 5.0, and 7.5 mol% ions, were synthesized by a hydrothermal process [23]. All chemicals were analytical grade reagents from Sigma-Aldrich (USA) and used as received. In a typical procedure, $Ba(NO_3)_2$, $ZrOCl_2$ $8H_2O$, and $Yb(NO_3)_3$ $5H_2O$ with the corresponding mole ratio of cations are completely dissolved in a 0.02 M CTAB ethanol-water solution (20 vol% ethanol) under vigorous stirring for 1 h at RT. Then, sodium hydroxide (0.5 M) was added and stirred again for 1 h at RT. The hydrothermal reactions were carried out in a Teflon autoclave

(500 mL) at 1000°C for 24 h. The precipitate was then washed with distilled water and dried in an oven at 1000°C for 15 h. This was further annealed at 1000°C for 14 h in air to remove organic materials and to enhance crystallinity. X-ray diffraction (XRD) patterns of as-prepared and annealed samples were obtained in a Siemens D-500 equipment equipped with a Cu tube with Kα radiation at 1.5405 Å, scanning in the 25° to 75° 2θ range at 0.02° steps and a sweep time of 8 s. SEM images were obtained in a XL30 JEOL equipment. The photoluminescence characterization and lifetime measurements were performed using two NIR excitation pump sources: 10 ns pulsed tunable Optical Parametric Oscillator (MOPO from Spectra Physics) pumped by the third harmonic of Nd: YAG pulsed laser and a 967 nm laser diode LDD-9A (from ATC semiconductor devices). The fluorescence emission was analyzed with an Acton Pro 500i monochromator and a R5509-73 Hamamatsu PMT connected to a SR830-DSP lock-in amplifier. Lifetimes were measured with a 500 MHz Lecroy oscilloscope. All photoluminescence measurements were performed at RT, and for VIS emissions a low band pass filter (cut off at 700 nm) was placed before the monochromator to prevent spurious excitation and its harmonics reaching the detector.

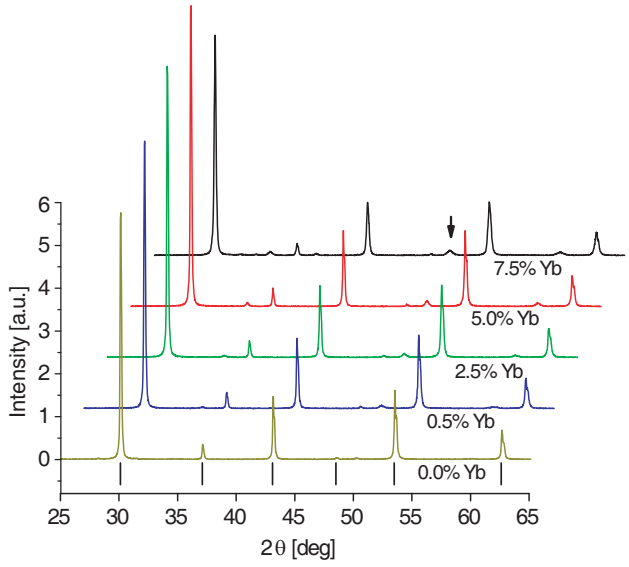

Figure 1. X-ray diffraction patterns of the as-synthesized $BaZrO_3$ (100°C) and Yb^{3+} doped $BaZrO_3$ annealed at 1000°C. Vertical bars at the bottom correspond to the JCPDS 6-0399 standard cubic perovskite $BaZrO_3$.

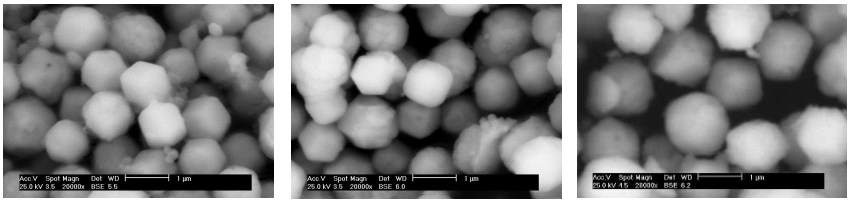

(a) (b) (c)

Figure 2. SEM micrographs of (a) undoped, (b) 1.0 and (c) 2.5 mol% Yb^{3+} samples annealed at 1000°C.

The XRD patterns of annealed BZO : Yb samples and undoped BZO (as-prepared) sample are shown in Figure 1. These patterns agree with JCPD-6-0399 standard for pure cubic perovskite $BaZrO_3$, with a lattice constant of 4.18°A. As the Yb^{3+} concentration increases, the degree of crystallinity increases, as revealed by the increase in intensity of the [1 1 0] reflection. When compared with undoped as-prepared BZO (at 100°C) no measurable differences can be observed. This confirms the high structural stability of the cubic phase of BZO, up to a 1000°C, and with doping concentrations as high as 2.5 mol% Yb^{3+}. The presence of additional reflections in the pattern for the 5.0 and 7.5 mol% Yb^{3+} samples (arrow) suggests segregation of other crystalline phases. Scherrer's equation gives crystallite sizes between 54 and 93 nm. Figure 2 shows typical SEM micrographs of undoped, 1.0 and 2.5 mol% Yb^{3+} samples annealed at 1000°. The observed morphologies correspond to well disperse secondary particles (i.e., aggregates) of around 750 nm, composed, in turn, by nanosized crystallites. For doping concentrations of 1.0 mol% Yb^{3+} and lower, the aggregates show well defined faceted morphologies, whereas for higher concentrations the morphology starts to switch to a spherical form. That is in agreement with the fact that segregation for high dopant concentration takes place and suggests that the segregation might be taking place at concentrations as low as 2.5 mol% Yb^{3+}.

The NIR emission spectra of all BZO : Yb^{3+} samples under excitation at 920 nm is shown in Figure 3(a). The spectra consist of two bands around 973 and 1032 nm, associated with the transition $^2F_{5/2} \rightarrow ^2 F_{7/2}$. Besides the NIR emission, strong blue-green emission was observed (Figure 3(c)). The VIS spectra between 450 nm and 580 nm (Figure 3(b)) correspond nearly to the half-wavelength range of the NIR emission from single Yb^{3+} ions. The best VIS emission corresponds to the 2.5 mol% Yb^{3+} sample, whereas the best NIR emission corresponds to the 0.5 mol% Yb^{3+} sample. The band at 502 nm almost corresponds to double energy of the infrared emission

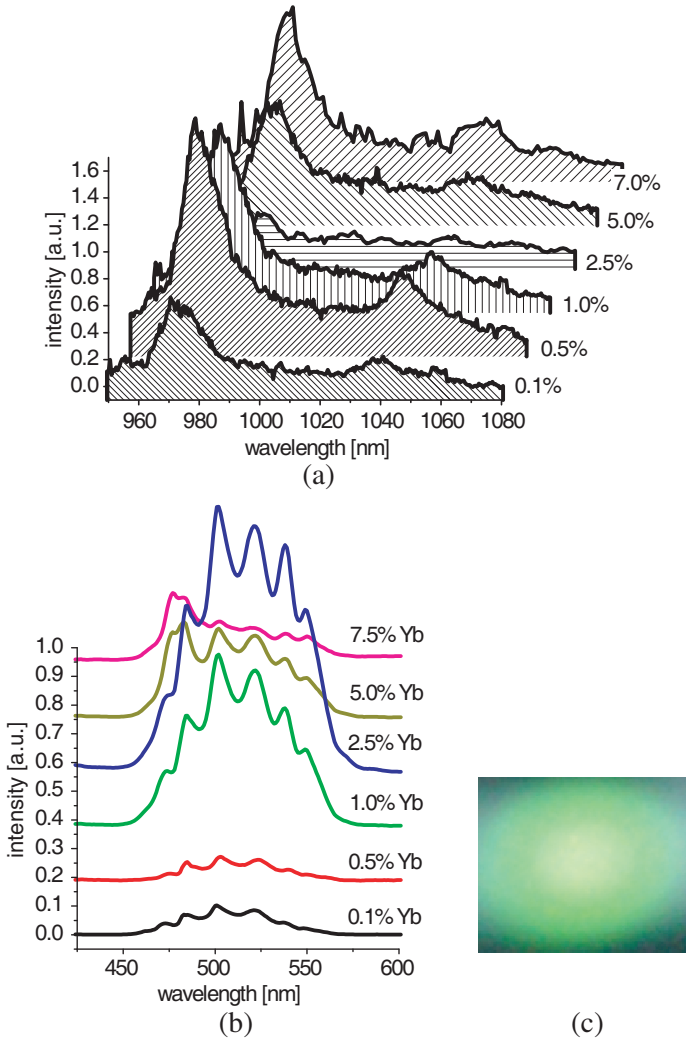

Figure 3. (a) NIR and (b) VIS emission spectra under 920 nm excitation of Yb^{3+} doped $BaZrO_3$. (c) Strong blue-green visible emission of 2.5 mol% Yb^{3+} doped $BaZrO_3$ under 920 nm excitation.

peak of 973 nm. The rest of the VIS peaks correspond to Er^{3+} and Tm^{3+} impurities emissions. Figure 4 shows the measured lifetimes of both 973 nm (circles) and 502 nm (squares) emission peaks. For all Yb^{3+} concentrations the visible lifetimes are almost half of the NIR lifetimes, suggesting that the emission at 502 nm is due to a cooperative up-conversion process among Yb^{3+} pair ions. This

behavior is similar to the report by Cannibano et al. for Yb^{3+} doped YAG, GGG and KBM hosts [24]. The relationship $I_{upc} = kI_{pump}^{n}$ between the upconverted intensity emission I_{upc} and pump intensity I_{pump} is broadly used to estimate the number of absorbed photons, n, required to produce an upconverted emission photon. The corresponding values of n for each Yb^{3+} concentration are plotted in Figure 4 (triangles). It is remarkable that n is almost constant with a value around 2. That supports the assumption that the up-conversion emission is a two-photon process due to the simultaneous de-excitation of two excited Yb^{3+} ions. Therefore, the green emission is due to a cooperative process among Yb^{3+} pairs. The observed visible luminescence (Figures 3(b) and 3(c)) is not completely originated by the cooperative emission between Yb^{3+} ions because of the presence of undesirable rare earth ions impurities in the precursor materials. The most likely impurities are erbium and thulium. Thus, the emissions in the visible range could also result from energy transfer processes from Yb^{3+} to Er^{3+} and/or Tm^{3+}. Such emissions can even mask the cooperative luminescence, provided that the impurity concentrations are high enough: See curves for 5.0 and 7.5 mol% Yb^{3+} in Figure 3(b). It is worth noticing that such impurities do not show detectable emission when excited directly in the UV-VIS range. Thus, it is likely that their emissions are basically due to energy transfer from the Yb^{3+} ions. The emissions peaks at 522 nm, 538 nm and 550 nm (Figure 3(b)) are characteristic of the ${}^{2}H_{11/2}+{}^{4}S_{3/2} \rightarrow {}^{4}I_{15/2}$ transition

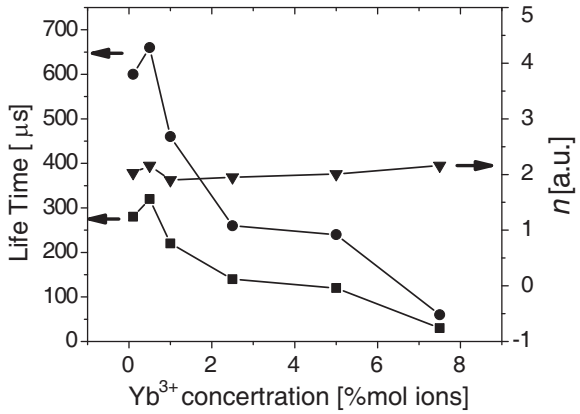

Figure 4. Dependence on Yb^{3+} concentration of the NIR and VIS emission life times, and dependence on the Yb^{3+} concentration for the number of NIR photons n needed to produce a VIS photon.

of Er^{3+} ion, due to the energy transfer from Yb^{3+} [6]. Thulium emission peaks at 474 nm and 484 nm, corresponding to the transition $^1G_4 \rightarrow {}^3H_6$, are also observed. Because the presence of Tm^{3+} and Er^{3+} impurities was not detected neither by absorption nor direct excitation, their concentration must be of the order of traces. Thus, the noticeable strong emission intensity at such low concentrations suggests very efficient energy transfer processes involving traces of Tm^{3+} and Er^{3+} ions having the Yb^{3+} ions as sensitizers.

That the observed reduction of both NIR and VIS life times as Yb^{3+} concentration increases (Figure 4) indicates the presence of quenching processes not related with the emission of the Er and Tm impurities, since their respective emissions are being quenched, as well. In Figures 3(a) and 3(b), it can be observed that both NIR and VIS emission bands are drastically reduced for concentrations above 2.5 mol% Yb^{3+} ions. With the increase of Yb^{3+} concentration, the separation between Yb-Yb pairs is reduced, promoting their interaction and thus enhancing the cooperative up-conversion emission at 502 nm, which on time reduces the NIR emission and promotes ET form Yb^{3+} pairs to Er^{3+} and Tm^{3+}, being the net result a reduction of both NIR and VIS emissions. Thus, the dominant effect is the Yb^{3+} pair interaction. It is presumed that if the Er^{3+} and Tm^{3+} ions concentrations are increased to nominal ones, then efficient ET process between Yb^{3+} and these ions could lead to strong emission in the blue (Tm^{3+}), green and red (Er^{3+}) regions. This would open the possibilities of BZO as a good phosphor for biolabeling applications [1, 2, 25, 26].

2. CONCLUSION

In conclusion, we have shown that Yb^{3+} doped $BaZrO_3$ as a up-conversion phosphor. BZO has very good structural and morphological characteristics and is stable in a wide range of annealing temperature and dopant concentrations. Yb^{3+} cooperative processes in BZO could be the base for new rare earth and transition metal doped phosphors for photonic applications in the VIS range under NIR excitation.

ACKNOWLEDGMENT

This work was partly supported by CONACYT trough grants 46971-F and 43168-F. J. Oliva also acknowledges CONACYT for a MSc scholarship at Centro de Investigaciones en Optica A.C.

REFERENCES

1. Chatterjee, D. K., A. J. Rufaihah, and Y. Zhang, "Upconversion fluorescence imaging of cells and small animals using lanthanide doped nanocrystals," *Biomaterials*, Vol. 29, 937–943, 2008.
2. Chen, G. Y., Y. G. Zhang, G. Somesfalean, and Z. G. Zhang, "Two-color upconversion in rare-earth-ion-doped ZrO_2 nanocrystals," *Appl. Phys. Lett.*, Vol. 89, 163105, 2006.
3. Filippov, V., Y. Chamorovskii, J. Kerttula, K. Golant, M. Pessa, and O. G. Okhotnikov, "Double clad tapered fiber for high power applications," *Opt. Express*, Vol. 16, No. 3, 1929, 2008.
4. Marchese, S. V., C. R. E. Baer, R. Peters, C. Kränkel, A. G. Engqvist, M. Golling, D. J. H. C. Maas, K. Petermann, T. Südmeyer, G. Huber, and U. Séller, "Efficient femtosecond high power $Yb:Lu_2O_3$ thin disk laser," *Opt. Express*, Vol. 15, No. 25, 16966, 2007.
5. Gangwar, R., S. P. Singh, and N. Singh, "L-band superfluorescent fiber source," *Journal of Electromagnetic Waves and Applications*, Vol. 21, No. 15, 2201–2204, 2007.
6. De la Rosa, E., P. Salas, L. A. Díaz-Torres, A. Martínez, and C. Angeles, "Strong visible cooperative up-conversion emission in $ZrO_2:Yb^{3+}$ Nanocrystals," *JNN*, Vol. 5, 1480, 2005.
7. Qin, G. S., W. P. Qin, C. F. Wu, D. Zhao, J. S. Zhang, S. Z. Lu, S. H. Huang, and W. Xu, "Infrared-to-visible upconversion luminescence of Er^{3+} and Yb^{3+} co-doped germanate glass," *J. Non-cryst Solids*, Vol. 347, 52, 2004.
8. Song, H. W., B. J. Sun, et al., "Three-photon upconversion luminescence phenomenon for the green levels in Er^{3+}/Yb^{3+} codoped cubic nanocrystalline yttria," *Solid State Commun.*, Vol. 132, 409, 2004.
9. Balda, R., A. J. Garcia-Adeva, M. Voda, and J. Fernandez, "Upconversion processes in Er^{3+}-doped KPb_2C_{15}," *Phys. Rev. B*, Vol. 69, 205203, 2004.
10. Auzel, F., "Upconversion and anti-stokes processes with f and d ions in solids," *Chem. Rev.*, Vol. 104, 139, 2004.
11. Suyver, J. F., A. Aebischer, D. Biner, P. Gerner, J. Grimm, S. Heer, K. W. Kramer, C. Reinhard, and H. U. Gudel, "Novel materials doped with trivalent lanthanides and transition metal ions showing near-infrared to visible photon upconversion," *Optical Materials*, Vol. 27, 1111, 2005.
12. Chen, G. Y., Y. Liu, Z. G. Zhang, B. Aghahadi, G. Somesfalean, Q. Sun, and F. P. Wang, "Four-photon upconversion induced

by infrared diode laser excitation in rare-earth-ion-doped Y_2O_3 nanocrystals," *Chemical Physics Letters*, Vol. 448, 127, 2007.

13. Sun, C. J., Z. Xu, B. Hu, G. S. Yi, G. M. Chow, and J. Shen, "Application of $NaYF_4 : Yb$, Er upconversion fluorescence nanocrystals for solution-processed near infrared photodetectors," *Appl. Phys. Lett.*, Vol. 91, 191113, 2007.
14. Jiang, L. Q., J. K. Guo, H. B. Liu, M. Zhu, X. Zhou, P. Wu, and C. H. Li, "Prediction of lattice constant in cubic perovskites," *J. Chem. Phys. of Solids*, Vol. 67, 1531, 2006.
15. Goodenough, J. B., "Electronic and ionic transport properties and other physical aspects of perovskites," *Rep. Prog. Phys.*, Vol. 67, 1915, 2004.
16. Patnaik, A. S. and A. V. Virka, "Transport properties of potassium-doped $BaZrO_3$ in oxygen- and water-vapor-containing atmospheres," *J. Electrochem. Soc.*, Vol. 153, No. 7, A1397, 2006.
17. Zeng, X., G. Zhao, and J. Xu, "Effects of Yb concentration on the fluorescence spectra of Yb-doped $YAlO_3$ single crystals," *Spectrochimica Acta. Part A*, Vol. 65, 184, 2006.
18. Amami, J., D. Hreniak, Y. Guyot, R. Pazik, C. Goutaudier, G. Boulon, M. Ayadi, and W. Strek, "Second harmonic generation and Yb^{3+} cooperative emission used as structural probes in size-driven cubic-tetragonal phase transition in $BaTiO_3$ sol-gel nanocrystals," *J. Lumin*, Vol. 383, 119–120, 2006.
19. Mattarelli, M., S. Sebastiani, J. Spirkova, S. Berneschi, M. Brenci, R. Calzolai, A. Chiasera, M. Ferrari, M. Montagna, G. Nunzi-Conti, S. Pelli, and G. C. Righini, "Characterization of erbium doped lithium niobate crystals and waveguides," *Opt. Mat.*, Vol. 28, 1292, 2006.
20. Hua, R. N., H. J. Sun, H. M. Jiang, and C. S. Shi, "Optical spectroscopy properties of $KMgF_3 : Eu^{2+}$ nanocrystals and powder synthesized by microemulsion and solvothermal," *Chem. Res. Chinese U.*, Vol. 22, No. 4, 423, 2006.
21. Sundell, P. G., M. E. Björketun, and G. Wahnström, "Thermodynamics of doping and vacancy formation in $BaZrO_3$ perovskite oxide from density functional calculations," *Phys. Rev. B*, Vol. 73, 104112, 2006.
22. Kang, S., A. Goyal, J. Li, A. A. Gapud, P. M. Martin, L. Heatherly, J. R. Thompson, D. K. Christen, F. A. List, M. Paranthaman, and D. F. Lee, "High-performance high-T_c superconducting wires," *Science*, Vol. 311, No. 31, 1911, 2006.
23. Shen, S. C., K. Hidajat, L. Y. E. Yu, and S. Kawi, "Simple

hydrothermal synthesis of nanostructured and nanorod Zn-Al complex oxides as novel nanocatalysts," *Adv. Mater.*, Vol. 16, No. 6, 541, 2004.

24. Canibano, E., "Propriétés spectroscopiques de l'ion Yb^{3+} dans les familles d'oxydes de molybdates K5Bi(MO4)4, de grenats Y3Al5O12, Gd3Ga5O12, Lu3Al5O12 et de perovskites YAlO3. Analyse de mécanismes d'extinction par concentration et évaluation de l'émission laser," PhD thesis, Université Claude Bernaud Lyon, France, 2002.
25. Lim, S. F., R. Riehn, W. S. Ryu, N. Khanarian, C.-K. Tung, D. Tank, and R. H. Austin, "In vivo and scanning electron microscopy imaging of upconverting nanophosphors in caenorhabditis elegans," *Nano Letters*, Vol. 6, No. 2, 169–174, 2006.
26. Goldys, E. M., K. Drozdowicz-Tomsia, G. Zhu, H. Yu, S. Jinjun, M. Motlan, and M. Godlewski, "Fluorescence labeling," *Optica Applicata*, Vol. 36, No. 2–3, 217–224, 2006.